JACC: BASIC TO TRANSLATIONAL SCIENCE
PUBLISHED BY ELSEVIER ON BEHALF OF THE AMERICAN COLLEGE OF CARDIOLOGY FOUNDATION.

VOL. 7, NO. 10, 2022

ORIGINAL RESEARCH - CLINICAL

Interstitial Collagen Loss, Myocardial Remodeling, and Function in Primary Mitral Regurgitation

Mustafa I. Ahmed, MD,[a,*] Efstathia Andrikopoulou, MD,[a,*] Jingyi Zheng, PhD,[c] Elena Ulasova, PhD,[b] Betty Pat, PhD,[a,d] Eric E. Kelley, PhD,[e] Pamela Cox Powell, MS,[a,d] Thomas S. Denney, Jr, PhD,[f] Clifton Lewis, MD,[g] James E. Davies, MD,[g] Victor Darley-Usmar, PhD,[b] Louis J. Dell'Italia, MD[a,d]

VISUAL ABSTRACT

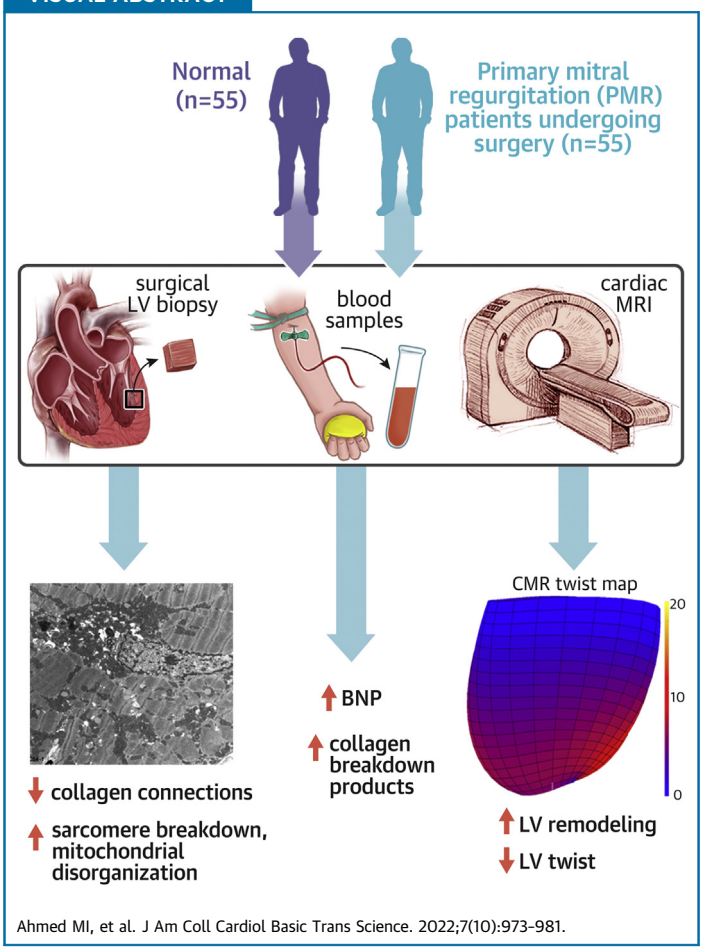

Ahmed MI, et al. J Am Coll Cardiol Basic Trans Science. 2022;7(10):973–981.

HIGHLIGHTS

- The stretch of volume overload in PMR initiates interstitial collagen loss and decrease in LV sphericity index.
- LV chamber diastolic function is normal whereas LA function, LV twist/volume slope, early LV untwist, and myocardial circumferential strain are impaired.
- There is increased oxidative stress in the cardiomyocyte with cytoskeletal breakdown and myofibrillar loss in PMR.

From the [a]Division of Cardiology, University of Alabama at Birmingham, Birmingham, Alabama, USA; [b]Department of Pathology, University of Alabama at Birmingham, Birmingham, Alabama, USA; [c]Department of Mathematics and Statistics, Auburn University, Auburn, Alabama, USA; [d]Birmingham Veterans Affairs Health Care System, Birmingham, Alabama, USA; [e]Department of Physiology and Pharmacology, West Virginia University, Morgantown, West Virginia, USA; [f]Samuel Ginn College of Engineering,

ISSN 2452-302X https://doi.org/10.1016/j.jacbts.2022.04.014

JACC: BASIC TO TRANSLATIONAL SCIENCE VOL. 7, NO. 10, 2022
OCTOBER 2022:973–981

ABBREVIATIONS AND ACRONYMS

BNP = brain natriuretic peptide

CMR = cardiac magnetic resonance

ED = end diastole

ES = end systole

ICTP = carboxy-terminal telopeptide of collagen type I

LA = left atrial

LV = left ventricle

LVEF = LV ejection fraction

PICP = carboxy-terminal propeptide of procollagen type I

PMR = primary mitral regurgitation

RV = right ventricle

SV = stroke volume

XO = xanthine oxidase

SUMMARY

Interstitial collagen loss and cardiomyocyte ultrastructural damage accounts for left ventricular (LV) sphericity and decrease in LV twist and circumferential strain. Normal LV diastolic function belies significantly abnormal left atrial (LA) function and early LV diastolic untwist rate. This underscores the complex interplay of LV and LA myocardial remodeling and function in the pathophysiology of primary mitral regurgitation. In this study, we connect LA function with LV systolic and diastolic myocardial remodeling and function using cardiac magnetic resonance tissue tagging in primary mitral regurgitation.

Chronic primary mitral regurgitation (PMR) results in a gradual progression of adverse eccentric left ventricular (LV) remodeling including a decrease in LV end-diastolic mass/volume ratio and radius/wall thickness and an increase in sphericity.[1] In the clinically relevant dog model of PMR, this adverse LV remodeling is associated with a decrease in interstitial collagen connecting cardiomyocytes.[2,3] However, studies using cardiac magnetic resonance (CMR) with T1 mapping and late gadolinium enhancement have inferred diffuse interstitial LV fibrosis in subjects with PMR.[4] There have been no studies evaluating the interstitial collagen content in the human PMR heart.

We have also reported an increase in cardiomyocyte xanthine oxidase (XO), extensive mitochondrial damage, and breakdown of desmin in patients with moderate to severe PMR and LV ejection fraction (LVEF) >60%.[5,6] Experts remain perplexed by the observation that LVEF may decrease to <50% in a subset of patients (20%) after surgery even with a presurgery LVEF >60%.[7-9] This has triggered interest into exploring other imaging parameters for timing of surgical intervention in PMR. CMR with tissue tagging provides LV myocardial strain by monitoring the motion of identifiable material points distributed throughout the myocardium.[5,6] In addition, left atrial (LA) remodeling and function has gained particular attention due to its central role and prognosis in the pathophysiology of PMR. Total LA emptying fraction and reservoir function provide predictive information equivalent to LV dimensions, LVEF, pulmonary artery pressure, LA volume, and effective orifice area combined[10] and predicts a decrease in LVEF after mitral valve surgery in PMR.[11,12]

We have previously reported in *JACC: Basic to Translational Science* that decreased total LA emptying fraction correlates with the extent of LA fibrosis in patients with PMR with LVEF >60%.[13] This underscores the complex interplay of LV and LA myocardial remodeling and function in the pathophysiology of PMR. In this study, we connect LA remodeling and function with LV systolic and diastolic myocardial remodeling and function using CMR tissue tagging in patients with PMR.

METHODS

PATIENT POPULATION. The study population included 55 normal controls and 55 presurgery patients with moderate to severe PMR before mitral valve surgery (**Table 1**). Patient recruitment occurred between 2006 and 2010 under National Heart, Lung, and Blood Institute Specialized Centers of Clinically Oriented Research Grant P50HL077100 in cardiac dysfunction. Patients with PMR had echo/Doppler severe isolated mitral regurgitation (MR) secondary to degenerative mitral valve disease referred for corrective mitral valve surgery. All patients had cardiac catheterization before surgery and were excluded for obstructive coronary artery disease (>50% stenosis), aortic valve disease, or mitral stenosis.[5,6]

Auburn University, Auburn, Alabama, USA; and the [g]Division of Thoracic and Cardiovascular Surgery, University of Alabama at Birmingham, Birmingham, Alabama, USA. *Drs Ahmed and Andrikopoulou contributed equally to this work.
The authors attest they are in compliance with human studies committees and animal welfare regulations of the authors' institutions and Food and Drug Administration guidelines, including patient consent where appropriate. For more information, visit the Author Center.

Manuscript received March 8, 2022; revised manuscript received April 27, 2022, accepted April 27, 2022.

Normal patients and patients with PMR had CMR with tissue tagging. Normal patients had no prior history of cardiovascular disease or medical illness, no history of smoking, and were not taking any cardiovascular medications. Control LV tissue (n = 51) for collagen picric acid Sirius red was obtained from nonfailing human hearts rejected for transplantation. The Institutional Review Boards of the University of Alabama at Birmingham and Auburn University approved the study protocol. All participants gave written informed consent.

CMR IMAGING. Normal patients and patients with PMR underwent CMR on a 1.5-T scanner (Signa, GE) with standard cardiac cine slices in 2- and 4-chamber views, and a short-axis view covering both ventricles and atria. Parameters were set as follows: field-of-view, 360-400 mm; 8-mm slice thickness; no gap; and 256*128 matrix. Tagged images were acquired using the same slice prescription as cine with the following parameters: repetition/echo times, 8/4.2 ms; tag spacing, 7 mm; trigger time, 10 ms from the R-wave; and flip angle, 10°.[1,5,6] In short-axis views, endocardial contours were manually drawn at end-diastole (ED) and end-systole (ES). In all patients, intersections of the mitral and tricuspid valve leaflets with the LV and right ventricular (RV) wall were manually placed in left 2- and 4-chamber view and a right 2-chamber view at ED and ES. All intersections and endocardial contours were propagated to the remaining time frames using an automated algorithm with excellent reproducibility. Mitral regurgitant volume was derived from the difference between LV and RV stroke volumes (SV). The 3-dimensional endocardial circumferential curvature and wall thickness were computed from standard formulas at the wall segments as previously defined in our laboratory.[1] LV twist (**Figure 1**) and shear angle parameters were computed using the Fourier Analysis of Stimulated echoes method.[14]

LA volumes were computed using biplane area-length method with manual contours on 2- and 4-chamber long-axis views for each time frame.[15] LA volumetric measurements were provided as maximum atrial volume (Vmax) when the mitral valve opens, minimum atrial volume (Vmin) when the mitral valve closes, and before atrial contraction volume (Vbac), measured at the time of peak LV late filling rate. Other LA functional parameters are calculated as follows:

- Total LA emptying fraction = (Vmax − Vmin)/Vmax × 100%
- LA reservoir function measured as LA expansion index = (Vmax − Vmin)/Vmin × 100%

TABLE 1 Demographics of Patients With PMR and Transthoracic Echo/Doppler (N = 55)

Medications	
None	17 (31)
Beta blocker	12 (22)
ACE inhibitor	13 (24)
AT_1 receptor blocker	3 (5)
Antiarrhythmic	3 (5)
Anticoagulant	2 (4)
Calcium entry blocker	4 (7)
Diuretic	13 (24)
Statins	4 (7)
NYHA functional class I	26 (47)
NYHA functional class II	27 (49)
NYHA functional class III	2 (4)
Diabetes mellitus	2 (4)
Hypertension	21 (38)
Atrial fibrillation	10 (18)
Transthoracic echo/Doppler	
LVEDD (mm)	54 ± 5
LVESD (mm)	35 ± 6
LVEF (%)	54 ± 4
LAD (mm)	44 ± 6
PASP Doppler (mm Hg)	41 ± 12
PASP indwelling catheter (mm Hg)	37 ± 13
PA wedge pressure (mm Hg)	18 ± 9
TR ≥2	15 (27)

Values are n (%) or mean ± SD.

ACE = angiotensin converting enzyme; LAD = left atrial dimension; LVEDD = left ventricular end diastolic dimension; LVEF = left ventricular ejection fraction; LVESD = left ventricular end systolic dimension; NYHA = New York Heart Association; PA = pulmonary artery; PASP = pulmonary artery systolic pressure; PMR = primary mitral regurgitation; TR = tricuspid regurgitation.

XO MEASUREMENT. Peripheral venous blood samples were centrifuged at 1,500*g* for 20 min at 4°C and stored at -80°C until analysis. XO activity is expressed as (μUnits) per mg total protein as previously performed in our laboratory.[16]

BRAIN NATRIURETIC PEPTIDE MEASUREMENT. Brain natriuretic peptide (BNP) was measured in plasma samples at the University of Alabama at Birmingham University Hospital Pathology laboratory (reference range: 0-100 pg/mL) and expressed as pg/mL.

COLLAGEN HOMEOSTASIS. Peripheral venous blood samples were immediately centrifuged at an equivalent of 1,500*g* for 20 min at 4°C and stored at -80°C. Carboxy-terminal propeptide of procollagen type I (PICP), a marker of type I collagen synthesis, was measured with a commercially available immunoassay (Quidel Corporation). Carboxy-terminal telopeptide of collagen type I (ICTP) levels, a marker of type I collagen degradation, were determined using immunoassay (Orion Diagnostic). Detection limits were 0.2 ng/mL for PICP and 0.3 ng/mL for ICTP.

FIGURE 1 LV Remodeling by CMR in Normal vs PMR

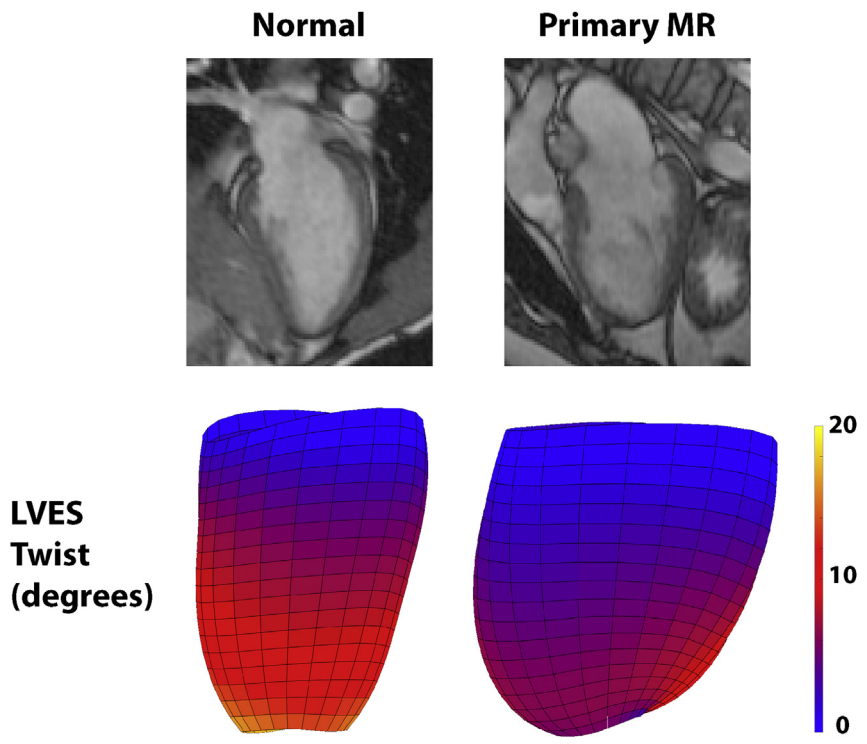

Two-chamber CMR images of normal control **(left)** and patient with PMR **(right)**. In the normal LV, twist (defined as rotation relative to base) values are 0 **(blue)** close to the base and change to **red** toward the apex, with **orange** denoting the largest twist at the apex. In the PMR heart, near the apex there is increased **blue** and **red** in the PMR, demonstrating a decrease in twist vs the normal heart. Septum is to the **left of each map**. CMR = cardiac magnetic resonance; LV = left ventricle; PMR = primary mitral regurgitation.

INTERSTITIAL COLLAGEN. LV endomyocardial biopsy specimens obtained at mitral valve surgery were immersion fixed in 3% paraformaldehyde.[2,3] Paraffin-embedded sections (3 μm) were stained with picric acid Sirius red F3BA. Interstitial collagen was identified using light microscopy at high power (40× objective; 1,600 total magnification). Percent collagen volume was quantified with a digital based image-analyzer system (Image-Pro Plus version 6.0, Media-Cybernetics) with the aid of a 540-nm (green) filter to provide grayscale contrast of the collagen with the background. A blinded analysis of percent collagen volume consisted of 10-15 randomly selected fields in each section with a mean value calculated for each patient as previously described in our laboratory.[2,3]

TRANSMISSION ELECTRON MICROSCOPY. Heart tissue was fixed overnight in 2.5% Glutaraldehyde in 0.1 mol/L sodium cacodylate buffer (Electron Microscopy Sciences) as previously described in our laboratory.[5,6] After postfixation with 1% osmium tetroxide in 0.1 mol/L cacodylate buffer, the tissue was dehydrated with a graded series of ethanol and embedded in Epon resin. Semi-thin and ultra-thin sections were cut, mounted on copper grids, and poststained with uranyl acetate and lead citrate. Sections were viewed in a transmission electron microscope for qualitative changes in mitochondria and cardiomyocyte ultrastructure.[5,6] To supplement the human studies, mechanistic studies were performed in a canine model of PMR.[2,3] The methods and results of these studies are presented in the Supplemental Material.

STATISTICS. Data are presented as number/total (%) in group (Table 1) or mean ± SD (Tables 2 to 4) or as box and whisker plots (graphs) with inner horizontal line as the median and the box indicating upper and lower quartiles and whiskers are the minimum and maximum values (Figures 2E and 2F). Data in Tables 2 to 4 were analyzed with Fisher exact test (2-sided) for categorical comparisons and the Wilcoxon rank sum test (Mann-Whitney) or unpaired Student's *t*-test for continuous comparisons depending on normality (Anderson-Darling, D'Agostino and Pearson, Shapiro-Wilk, and Kolmogorov-Smirnov tests). A value of $P < 0.05$ was considered to be statistically significant.

Analyses were performed in GraphPad Prism 9.3.0. Results should be interpreted with caution as comparisons were not adjusted for type I errors.

RESULTS

DEMOGRAPHICS OF THE PATIENTS WITH PMR. Table 1 summarizes medications, comorbidities, and Doppler echocardiographic characteristics in patients with PMR. There is an 18% incidence of episodic atrial fibrillation, a 38% history of hypertension, and a 27% incidence of ≥2+ tricuspid regurgitation based on echo/Doppler study. Most patients are Class I (47%) and Class II (49%). The mean value of Doppler estimated and invasive hemodynamic pulmonary artery pressures are 41 ± 12 mm Hg and 37 ± 13 mm Hg, respectively.

CHARACTERIZATION OF LV REMODELING. Mean LVEF is 63% ± 8% in patients with PMR, which does not differ from normal controls (64% ± 5%) (Table 2). However, left ventricular end-diastolic volume, LVSV, left ventricular end-diastolic dimension, regurgitant volume, and fraction are consistent with moderate to severe MR. An increase in 3-dimensional endocardial LVED mid-LV radius of curvature to wall thickness ratio is consistent with a significant decrease in the LVED mass/volume ratio and sphericity index compared with normal. Figure 1 demonstrates spherical LVED remodeling in PMR from mid-wall to apex and a decrease in LV systolic twist/volume slope. LVES diameter (mm) and LVES volume (mL/m^2) and BNP are increased, whereas LVED mass/volume is decreased compared with normal. In addition, there is a shift of laminar plane orientation demonstrating a global increase in angles between principal strain directions and normal strain in circumferential, longitudinal, and radial directions (Table 3).

MYOCARDIAL INTERSTITIAL COLLAGEN AND CIRCULATING BIOMARKERS. LV endocardial biopsy samples demonstrated an increase in interstitial space that is devoid of collagen based on Picric acid Sirius red staining with patchy fibrosis in areas of cardiomyocyte loss (Figures 2A to 2D). There is a spectrum of interstitial collagen scores in PMR, with many decreasing below the median normal cutoff (3.5%) (Figure 2F). The increase in ICTP (Table 2), a marker of collagen degradation, and the decreased plasma PICP:ICTP ratio in PMR (Figure 2E) support a disproportionate increase in collagen degradation over synthesis in PMR.

TRANSMISSION ELECTRON MICROSCOPY IN THE HUMAN PMR. Figure 3 demonstrates transmission electron micrographs (4,000×) in 3 patients with PMR with CMR-derived LVEF of 72% (Figure 3A), 63% (Figure 3B), and 62% (Figure 3C), demonstrating multiple areas of myofibril breakdown with small, disorganized mitochondria in areas of sarcomere breakdown and numerous empty vacuoles of lipid droplets (L) in the myocyte.

TABLE 2 PMR Demographics and CMR Data

	Normal (n = 55)	Presurgery PMR (n = 55)	*P* Value
Age, y	45 ± 14	56 ± 12	<0.001
Female/male	31 (56)/24 (44)	16 (29)/39 (71)	0.007
Black/white	20 (36)/33 (60)	6 (11)/47 (85)	0.003
BMI, kg/m^2	26 ± 6	27 ± 5	0.52
BSA, m^2	1.9 ± 0.3	2.0 ± 0.2	0.27
LVEF, %	64 ± 5	63 ± 8	0.77
LVED volume, mL/m^2	69 ± 11	109 ± 24	<0.001
LVES volume, mL/m^2	25 ± 6	40 ± 13	<0.001
LV stroke volume, mL/m^2	44 ± 7	69 ± 18	<0.001
LVED diameter, mm	50 ± 5	58 ± 7	<0.001
LVES diameter, mm	36 ± 4	45 ± 7	<0.001
LVED mass/volume, g/mL	0.74 ± 0.17	0.66 ± 0.14	0.005
LV SI	1.79 ± 0.21	1.59 ± 0.24	<0.001
LVED radius/wall thickness	3.83 ± 0.84	4.50 ± 0.99	<0.001
Regurgitant volume, mL	–	64 ± 32	
BNP, pg/mL	8.3 ± 10.3	80.0 ± 104	<0.001
XO activity, μU/mg[a]	0.021 ± 0.039	0.031 ± 0.028	<0.001
PICP	96 ± 48	86 ± 37	0.25
ICTP	3.1 ± 1.3	4.4 ± 3.4	0.038
PICP:ICTP	34 ± 15	26 ± 16	0.006

Values are mean ± SD or n (%). [a]XO normalized to protein in plasma.

BMI = body mass index; BNP = brain natriuretic peptide; BSA = body surface area; CMR = cardiac magnetic resonance; ICTP = carboxy-terminal telopeptide of collagen type I; LV = left ventricular; LVED = LV end-diastolic; LVES = LV end-systolic; PICP = carboxy-terminal propeptide of procollagen type I; SI = Sphericity Index; XO = xanthine oxidase; other abbreviations are as in Table 1.

LA FUNCTION AND LV REMODELING AND FUNCTION FROM MYOCARDIAL TISSUE TAGGING. MR LA maximum and minimum volumes are increased nearly 2- and 3-fold vs normal controls (Table 4). There is a significant decrease in expansion index and total LA emptying fraction. In contrast, normalized early peak LV diastolic filling rates, peak early diastolic mitral annular velocity (e', mm/s), and normalized peak early diastolic mitral annular velocity are completely within normal limits.

Myocardial tissue tagging was used to study LV myocardial function. Peak early diastolic circumferential and longitudinal strain rate (%/s) did not differ in PMR and normals. However, peak early diastolic normalized untwist rate (adjusted to diastolic interval) was significantly decreased compared with normals. Peak LV systolic twist remain unchanged, however, peak LV systolic twist/volume slope was decreased compared with normal. Mid-LV circumferential strain and not longitudinal strain was decreased to less than normal.

TABLE 3 Angles Between Principal Strain Directions and Normal Strain (Circumferential, Longitudinal, and Radial) Directions

	Base			Mid			Apex		
	Normal	PMR	*P* Value	Normal	PMR	*P* Value	Normal	PMR	*P* Value
Ecc angle,°	42.98 ± 6.97	46.53 ± 8.32	**0.017**	34.25 ± 5.59	41.25 ± 9.13	**<0.001**	36.82 ± 7.29	43.15 ± 9.25	**<0.001**
Ell angle,°	47.83 ± 7.80	52.01 ± 8.76	**0.001**	36.44 ± 6.56	42.01 ± 9.15	**<0.001**	40.66 ± 7.09	42.89 ± 8.78	0.22
Err angle,°	21.07 ± 8.02	23.84 ± 7.41	**0.035**	15.72 ± 7.08	16.77 ± 6.12	0.26	24.82 ± 10.45	24.15 ± 10.58	0.67

Values are mean ± SD. N = 55 for both normal and MR groups. Values in **boldface** are significant.
Ecc = circumferential strain angle; Ell = longitudinal strain angle; Err = radial strain angle.

DISCUSSION

CONSEQUENCES OF LOSS OF INTERSTITIAL COLLAGEN ON LV REMODELING IN PMR. The contiguous collagen framework of the heart encompasses epimysial, perimysial, and endomysial collagen. In our patients with PMR, PASR staining shows a loss of endomysial collagen between cardiomyocytes and a decrease in plasma PICP:ICTP ratio. The loss of collagen supporting structure explains the spherical LV remodeling and a decrease in global rotational shortening dynamics.[17] The decrease in the LV sphericity index is associated with a shift of laminar plane orientation with a global increase in angles between principal strain directions and normal strain in circumferential, longitudinal, and radial directions (Table 3). In dog models of PMR and aortocaval fistula, shifts in laminar architecture coincide with transition to a more spherical LV and decrease in LV twist despite LVEF >60%.[18,19]

TABLE 4 CMR of LA and LV Function

	Normal (n = 51)	PMR (n = 55)	*P* Value
CMR LA Function			
LA max, mL/m^2	31 ± 8	63 ± 22	<0.001
LA min, mL/m^2	14 ± 4	36 ± 17	<0.001
LA expansion index, %	123 ± 39	85 ± 40	<0.001
LA total emptying fraction, %	54 ± 7	44 ± 11	<0.001
CMR LV Chamber Diastolic Function			
	(n = 55)	(n = 55)	
Normalized peak LV early diastolic filling rate (E), EDV/s	2.8 ± 0.7	2.8 ± 0.7	0.96
Normalized peak late diastolic filling rate (A), EDV/s	1.6 ± 0.6	1.4 ± 0.4	0.02
E/A ratio	2.4 ± 3.0	2.3 ± 1.1	0.85
Peak early diastolic MA velocity (e'), mm/s	-7.4 ± 2.6	-7.5 ± 2.3	0.69
Normalized peak early diastolic MA velocity, % long axis length/s	-83 ± 28	-82 ± 24	0.84
CMR With Tissue Tagging LV Myocardial Diastolic Function			
	(n = 55)	(n = 55)	
Peak early diastolic circumferential strain rate, %/s	0.95 ± 0.32	1.03 ± 0.31	0.17
Peak early diastolic longitudinal strain rate, %/s	1.10 ± 0.64	1.17 ± 0.48	0.21
Peak early diastolic untwist rate, °/cm	-0.015 ± 0.006	-0.013 ± 0.004	0.01
Time to peak untwist rate, ms	387 ± 41	395 ± 49	0.34
CMR With Tissue Tagging LV Myocardial Systolic Function			
	(n = 55)	(n = 55)	
Peak LV twist, °	14.3 ± 3.5	14.1 ± 4.5	0.84
LV systolic twist/Vol slope, °/mL	-0.126 ± 0.045	-0.073 ± 0.031	<0.001
Mid-LVES circumferential strain	-0.16 ± 0.02	-0.14 ± 0.03	0.001
Mid-LVES longitudinal strain	-0.12 ± 0.02	-0.12 ± 0.03	0.75

Values are mean ± SD.
LA = left atrial; MA = mitral annular; Vol = LV stroke volume; other abbreviations as in Table 2.

Twist is the LV wringing motion along its long axis during systole induced by contracting myofibers connected by collagen that are aligned 180° from the endocardium to epicardium. In our patients with PMR, twist per volume slope decreases along with mid-LV circumferential strain. The increase in 3-dimensional radius of curvature wall thickness reflects an increase in wall stress, consistent with the 10-fold increase in plasma BNP (Table 2). The potential importance of circumferential strain in PMR is consistent with models that determine the effect of LV shape on LVEF, where circumferential strain is significantly more important than longitudinal strain in maintaining LVEF in the spherically dilated LV.[20]

LA REMODELING AND FUNCTION. We have reported decreased total LA emptying fraction that correlates with the extent of LA fibrosis in patients with PMR with LVEF >60%.[13] In addition to LA size alone,[21,22] indices of LA function have shown important prognostic capabilities underscoring that the left atrium is not simply a passive conduit.[10-12] Here we demonstrate a marked increase in LA volumes, a decrease in total LA emptying fraction, and a 50% decrease in LA expansion index. These indices of poor LA function and compliance increase pulmonary vascular resistance and RV afterload. In a study of 1,318 patients with moderate to severe PMR, LVEF >60% and LVES diameter <4.0 cm, the addition of RV systolic pressure >35 mm Hg is an independent predictor of shortened survival and adds predictive accuracy to the Society of Thoracic Surgeons Score.[23]

LV CHAMBER AND MYOCARDIAL DIASTOLIC FUNCTION IN PMR. Previous studies of patients with PMR with simultaneous LV biplane cine-angiography and high-

FIGURE 2 **PASR Staining From LV Endomyocardial Biopsies in PMR**

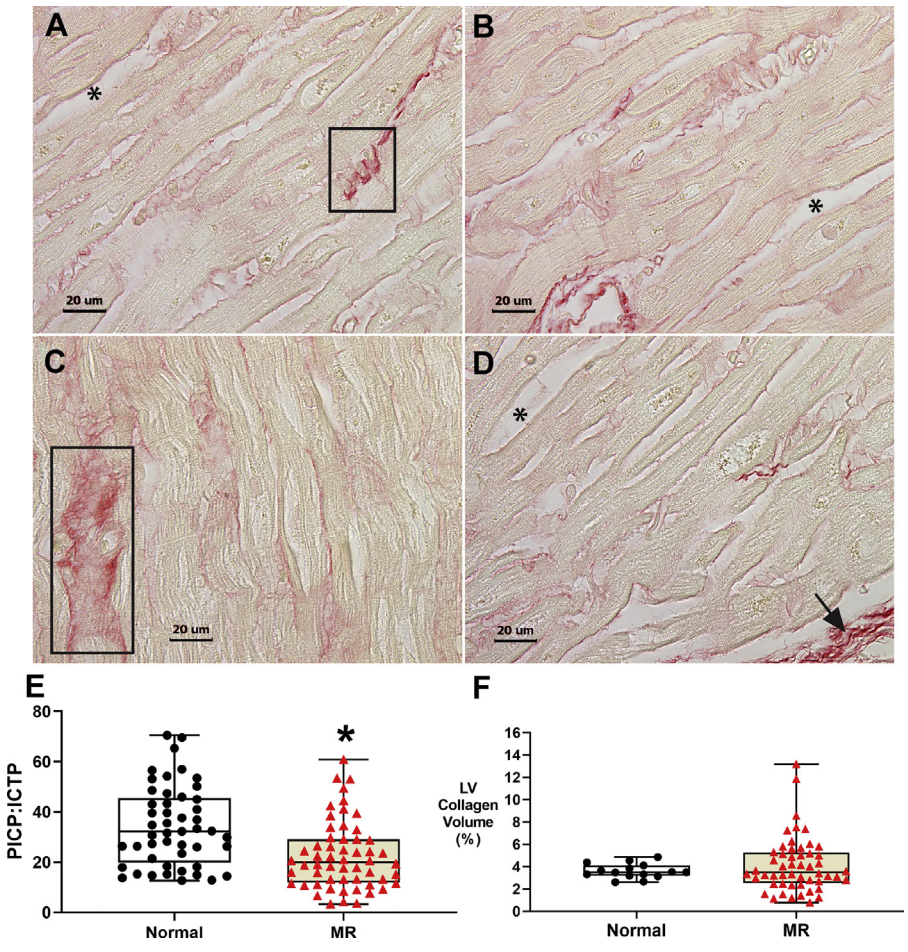

(A to D) Multiple areas of interstitial space devoid of collagen **(*)**. **(A and B)** Areas of patchy replacement fibrosis **(red)** of dying cardiomyocytes **(black boxes)**. Endocardial portion of the biopsy **(black arrow in D)**. **(E)** PICP:ICTP ratio decreases in presurgical PMR patients vs normal controls. **(F)** PASR quantitation of LV interstitial collagen in tissue biopsies does not differ in patients with PMR vs age-matched nonfailing (control) hearts. *$P < 0.001$ vs normal based on Wilcoxon rank sum test (Mann-Whitney). Data presented as box and whisker plots of median and IQR. Each symbol **(circles or triangles)** is an individual patient. ICTP = carboxy-terminal telopeptide of collagen type I; PASR = Picric Acid Sirius Red; PICP = carboxy-terminal propeptide of procollagen type I.

fidelity LV pressures demonstrate decreased LV myocardial stiffness and increased LV chamber compliance in patients with PMR with normal LVEF, whereas increased myocardial stiffness occurs only in patients with LVEF <50%.[24] In the dog with chronic PMR, Zile et al[25] demonstrate that coincident with a decrease in LV chamber stiffness constant, there is a significant increase in the pulmonary capillary wedge pressure to LV end-diastolic pressure gradient that drives the increase in LV filling.[25] In addition, they show a decrease in the lengthening rate of isolated dog PMR cardiomyocytes, suggesting a decrease in restoring forces.[26] In our patients with PMR, all indices of LV diastolic filling, peak early diastolic circumferential strain rate (%/s), and peak early diastolic longitudinal strain rate (%/s) are normal, except for the peak early diastolic untwist rate. Using speckle-tracking echocardiography, which offers a higher sampling frequency, there is a significant delay in peak of LV untwisting velocity in chronic PMR.[27] Thus, the increase in LA pressure caused by fibrosis and decrease in distensibility play a major role in maintaining early LV diastolic filling. Untwist rate may represent an early manifestation of LV myocardial diastolic dysfunction in PMR. Importantly, LA myocyte ultrastructural damage and fibrosis connect total LA emptying fraction to pulmonary vascular resistance, shortness of breath, and atrial fibrillation.

FIGURE 3 Transmission Electron Microscopy of the LV in Patients With PMR

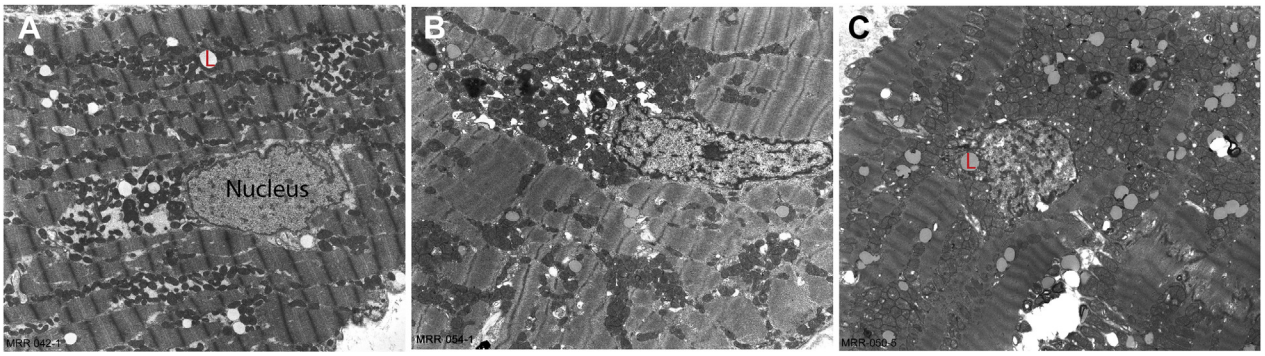

Patients with PMR with CMR LVEF of **(A)** 72%, **(B)** 63%, and **(C)** 62%. There is extensive myofibrillar breakdown with small, disorganized mitochondria in areas of sarcomere breakdown with numerous lipid droplets (L). LVEF = left ventricular ejection fraction.

COMPARISON OF HUMAN STUDIES OF PMR TO A CANINE MODEL OF PMR. There is a similar increase in LV XO activity and decrease in interstitial collagen in the dog and human with PMR, along with marked myofilament lysis and mitochondrial damage (Supplemental Figures 1 and 2). Products of XO, superoxide and hydrogen peroxide, can negatively influence multiple targets, either independently or after reaction with molecules including nitric oxide ($O_2^{\bullet-}$ + $^{\bullet}NO$ O=NOO-). XO depresses myofilament sensitivity to calcium and colocalizes with nitric oxide synthase-1 and the ryanodine receptor in the cardiomyocyte sarcoplasmic reticulum.[28,29] In addition, messenger RNA and protein levels of the sarcoplasmic reticulum Ca^{2+} adenosine triphosphatase-negative regulatory protein sarcolipin, which is predominantly expressed in the atria, are increased 12- and 6-fold in patients with PMR, respectively. In this microenvironment, the deleterious effects of cardiomyocyte XO can negatively influence excitation contraction coupling and lengthening, as well as promote myofilament lysis, and post-translational modification of cytoskeletal and contractile proteins.[30] This combined with collagen loss (Supplemental Figure 2) can mediate cardiomyocyte elongation and thinning, LV spherical remodeling, decrease in mid-LV circumferential strain, and global decrease in LV twist and untwist—all masked by LVEF >60% caused by ejection into the low pressure left atrium.

STUDY LIMITATIONS. The results of this study should be interpreted with caution as comparisons were not adjusted for type I errors. There is very little known about the "physiologic progression" of PMR. Thus, futures studies utilizing a longitudinal study design with traditional regression and/or machine learning methods or a combination of both will allow for better integration of inflammatory biomarkers and CMR derived LA and LV parameters to identify new predictors of symptoms and LVEF <60% in asymptomatic PMR and better timing for mitral valve surgery.

CONCLUSIONS

Twenty percent of patients with PMR have an increased chance of LVEF <50% after mitral valve repair despite presurgical LVEF >60%.[6-8] Here, in patients with PMR with LVEF >60% and Class I (47%) or Class II (49%) status, we show that indices of LV sphericity and circumferential myocardial strain combined with LA remodeling and function may provide early indicators for surgery in asymptomatic to minimally symptomatic patients with PMR with LVEF >60%.

FUNDING SUPPORT AND AUTHOR DISCLOSURES

This work was supported by the National Heart, Lung, and Blood Institute and Specialized Centers of Clinically Oriented Research grant (P50HL077100 to Dr Dell'Italia) in cardiac dysfunction; R01 DK124510-01, R01 HL153532-01A1, and AHA 19TPA34850089 (to Dr Kelley); Department of Veteran Affairs for Merit Review grant (1CX000993-01 to Dr Dell'Italia); and National Institutes of Health grant (P01 HL051952 to Dr Dell'Italia). All other authors have reported that they have no relationships relevant to the contents of this paper to disclose.

ADDRESS FOR CORRESPONDENCE: Dr Louis J. Dell'Italia, Birmingham VA Health Care System, 700 South 19th Street, Birmingham, Alabama 35233, USA. E-mail: louis.dellitalia@va.gov.

PERSPECTIVES

COMPETENCY IN MEDICAL KNOWLEDGE: An understanding of the underlying mechanisms of LA and LV remodeling in the pathophysiology of PMR may identify an appropriate time for surgical repair of the mitral valve.

TRANSLATIONAL OUTLOOK: Timing for surgical intervention in PMR is currently unclear and fraught with a 20% chance for a decrease in LVEF less than normal, after surgical repair of the valve. This work provides the impetus for future longitudinal studies that use CMR-derived LV and LA remodeling and function with biomarkers to define optimal surgical timing in patients with PMR.

REFERENCES

1. Schiros CG, Dell'Italia LJ, Gladden JD, et al. Magnetic resonance imaging with 3-dimensional analysis of left ventricular remodeling in isolated mitral regurgitation: implications beyond dimensions. *Circulation*. 2012;125:2334–2342.

2. Zheng J, Chen Y, Pat B, et al. Microarray identifies extensive downregulation of noncollagen extracellular matrix and profibrotic growth factor genes in chronic isolated MR in the dog. *Circulation*. 2009;119:2086–2095.

3. Dell'Italia LJ, Balcells E, Meng QC, et al. Volume overload cardiac hypertrophy is unaffected by ACE inhibitor treatment in the dog. *Am J Physiol*. 1997;273:H961–H970.

4. Kitkungvan D, Yang EY, El Tallawi KC, et al. Extracellular volume in primary mitral regurgitation. *J Am Coll Cardiol Img*. 2021;14(6):1146–1160.

5. Ahmed MI, Gladden JD, Litovsky SH, et al. Increased oxidative stress and cardiomyocyte myofibrillar degeneration in patients with chronic isolated mitral regurgitation and ejection fraction >60%. *J Am Coll Cardiol*. 2010;55:671–679.

6. Ahmed MI, Guichard JL, Soorappan RN, et al. Disruption of desmin-mitochondrial architecture in patients with regurgitant mitral valves and preserved ventricular function. *J Thorac Cardiovasc Surg*. 2016;152:1059–1070.

7. Otto CM, Nishimura RA, Bonow RO, et al. ACC/AHA guideline for the management of patients with valvular heart disease: a report of the ACC/AHA Joint Committee on Clinical Practice Guidelines. *J Am Coll Cardiol*. 2020:S0735–S1097.

8. Miller JD, Suri RM. Left ventricular dysfunction after degenerative mitral valve repair: a question of better molecular targets or better surgical timing? *J Thorac Cardiovasc Surg*. 2016;152(4):1071–1074.

9. Quintana E, Suri RM, Thalji NM, et al. Left ventricular dysfunction after mitral valve repair-the fallacy of "normal" preoperative myocardial function. *J Thorac Cardiovasc Surg*. 2014;148:2752–2762.

10. Zito C, Manganaro R, Khandheria B, et al. Usefulness of left atrial reservoir size and left ventricular untwisting rate for predicting outcome in primary mitral regurgitation. *Am J Cardiol*. 2015;116(8):1237–1244.

11. Ring L, Rana BS, Wells FC, Kydd AC, Dutka DP. Atrial function as a guide to timing of intervention in mitral valve prolapse with mitral regurgitation. *J Am Coll Cardiol Img*. 2014;7(3):225–232.

12. Kislitsina ON, Thomas JD, Crawford E, et al. Predictors of left ventricular dysfunction after surgery for degenerative mitral regurgitation. *Ann Thorac Surg*. 2020;109(3):669–677.

13. Butts B, Ahmed MI, Powell PC, et al. Left atrial emptying fraction and chymase activation in the pathophysiology of primary mitral regurgitation. *J Am Coll Cardiol Basic Trans Science*. 2020;5(2):109–122.

14. Reyhan M, Wang Z, Li M, et al. Left ventricular twist and shear in patients with primary mitral regurgitation. *J Magn Reson Imaging*. 2015;42(2):400–406.

15. Schiros CG, Ahmed MI, McGiffin DC, et al. Mitral annular kinetics, left atrial, and left ventricular diastolic function post mitral valve repair in degenerative mitral regurgitation. *Front Cardiovasc Med*. 2015;17:31.

16. Butts B, Calhoun DA, Denney TS Jr, et al. Plasma xanthine oxidase activity is related to increased sodium and left ventricular hypertrophy in resistant hypertension. *Free Radic Biol Med*. 2019;134:343–349.

17. Pope AJ, Sands GB, Smaill BH, LeGrice IJ. Three-dimensional transmural organization of perimysial collagen in the heart. *Am J Physiol*. 2008;295:H1243–H1252.

18. Ashikaga H, Omens JH, Covell JW. Time-dependent remodeling of transmural architecture underlying abnormal ventricular geometry in chronic volume overload heart failure. *Am J Physiol*. 2004;287(5):H1994–H2002.

19. Ennis DB, Nguyen TC, Itoh A, et al. Reduced systolic torsion in chronic "pure" mitral regurgitation. *Circ Cardiovasc Imaging*. 2009;2:85–92.

20. Stokke TM, Hasselberg NE, Smedsrud MK, et al. Geometry as a confounder when assessing ventricular systolic function. Comparison between ejection fraction and strain. *J Am Coll Cardiol*. 2017;70(8):942–954.

21. Le Tourneau T, Messika-Zeitoun D, Russo A, et al. Impact of left atrial volume on clinical outcome in organic mitral regurgitation. *J Am Coll Cardiol*. 2010;56(7):570–578.

22. Rusinaru D, Tribouilloy C, Grigioni F, et al. Mitral Regurgitation International DAtabase (MIDA) Investigators. Left atrial size is a potent predictor of mortality in mitral regurgitation due to flail leaflets: results from a large international multicenter study. *Circ Cardiovasc Imaging*. 2011;4(5):473–481.

23. Mentias A, Patel K, Patel H, et al. Effect of pulmonary vascular pressures on long-term outcome in patients with primary mitral regurgitation. *J Am Coll Cardiol*. 2016;28;67(25):2952–2961.

24. Corin WJ, Murakami T, Monrad ES, Hess OM, Krayenbuehl HP. Left ventricular passive diastolic properties in chronic mitral regurgitation. *Circulation*. 1991;83(3):797–807.

25. Zile MR, Tomita M, Nakano K, et al. Effects of left ventricular volume overload produced by mitral regurgitation on diastolic function. *Am J Physiol*. 1991;261(5 Pt 2):H1471–H1480.

26. Tsutsui H, Urabe Y, Mann DL, et al. Effects of chronic mitral regurgitation on diastolic function in isolated cardiocytes. *Circ Res*. 1993;72(5):1110–1123.

27. Borg AN, Harrison JL, Argyle RA, Ray SG. Left ventricular torsion in primary chronic mitral regurgitation. *Heart*. 2008;94(5):597–603.

28. Khan SA, Skaf MW, Harrison RW, et al. Neuronal nitric oxide synthase negatively regulates xanthine oxidoreductase inhibition of cardiac excitation-contraction coupling. *Proc Natl Acad Sci U S A*. 2004;101:15944–15948.

29. Perez NG, Gao WD, Marban E. Novel myofilament Ca2+ -sensitizing property of xanthine oxidase inhibitors. *Circ Res*. 1998;83:423–430.

30. Zheng J, Yancey DM, Ahmed MI, et al. Increased sarcolipin expression and adrenergic drive in humans with preserved left ventricular ejection fraction and chronic isolated mitral regurgitation. *Circ Heart Fail*. 2014;7(1):194–202.

KEY WORDS cardiac magnetic resonance, collagen loss, left ventricular remodeling, primary mitral regurgitation

APPENDIX For supplemental data and figures, please see the online version of this paper.